

Preferential growth of SmBCO on Sm211 whiskers and its dependence upon supersaturation

This article has been downloaded from IOPscience. Please scroll down to see the full text article.

2005 J. Phys.: Condens. Matter 17 4731

(<http://iopscience.iop.org/0953-8984/17/30/001>)

View [the table of contents for this issue](#), or go to the [journal homepage](#) for more

Download details:

IP Address: 129.252.86.83

The article was downloaded on 28/05/2010 at 05:39

Please note that [terms and conditions apply](#).

Preferential growth of SmBCO on Sm211 whiskers and its dependence upon supersaturation

Xinhua Zeng¹ and Xin Yao^{1,2}

¹ Department of Physics, Shanghai Jiao Tong University, People's Republic of China

² State Key Laboratory for Metal Matrix Composites, Shanghai Jiao Tong University, People's Republic of China

Received 25 April 2005, in final form 10 June 2005

Published 15 July 2005

Online at stacks.iop.org/JPhysCM/17/4731

Abstract

The process of epitaxial growth of the SmBCO phase on the surface of the Sm211 whisker via the peritectic reaction $\text{Sm211} + \text{L} \rightarrow \text{SmBCO}$ was first observed *in situ* by high temperature optical microscopy. A preferential epitaxial relation between the SmBCO and Sm211 was demonstrated. From the bonding energy point of view, it was suggested that both 0° and 45° epitaxial relations between them are appropriate. A schematic illustration as regards the growth dependence of 0° and 45° oriented SmBCO on the supersaturation was proposed to illustrate the growth competition between these two types of SmBCO on Sm211 whiskers in this work.

(Some figures in this article are in colour only in the electronic version)

1. Introduction

$\text{REBa}_2\text{Cu}_3\text{O}_y$ (REBCO or RE123) thick films and coated conductors may be grown epitaxially directly on some gallate substrate materials, such as NdGaO_3 , LaGaO_3 and LaSrGaO_4 [1–4], while for most other substrate materials, e.g., LaAlO_3 , SrTiO_3 , MgO , NiO , Ag and yttrium stabilized ZrO_2 (YSZ), a thin film seed layer is indispensable [5–10]. Asaoka *et al* found that the RE123 phase can be formed around the $\text{RE}_2\text{BaCuO}_5$ (RE211) phase, and Sandiumenge showed some SAD patterns that indicated parallelism between crystallographic directions of the Y211 precipitate and the Y123 matrix, i.e. RE211 crystals may act as nuclei for the direct liquid phase epitaxy (LPE) growth of REBCO [11, 12]. There will be at least two major potential applications if this conclusion can be confirmed. On one hand, RE211 crystals could be applied as candidate seeds for the melt-textured growth (MTG) of REBCO bulks. There will be some advantages over the conventional seeds used for MTG of REBCO bulks, e.g., a higher melting point than for REBCO seeds and no introduction of deleterious elements like REBCO. On the other hand, there is also potential for application in the area of coated conductors. REBCO coated conductors cannot grow epitaxially on metallic tapes. In order to prevent contamination and solve the misfit problem, a multi-layered structure is usually suggested [13]. It is very difficult to achieve such coated conductors because there are generally

more than four layers of the metallic superconductor tape. A buffer layer can be omitted if the REBCO phase can be grown epitaxially on the RE211 buffer layer. Compared to other buffer layers, RE211 phase buffer layer is contamination free. However, Nishimura *et al* had the opposite opinion: that the RE211 particles did not play an active role in the nucleation of RE123 crystals [14]. Confirmation of this relation may provide some potential applications for 211, such as seeding growth of REBCO single crystals or MT bulks, and application as a novel seed film or substrate for REBCO coated conductors.

In our previous work [15, 16], we used an elaborate method to obtain some $\text{Sm}_2\text{BaCuO}_5$ (Sm211) whiskers several millimetres in length. The characterization of such Sm211 whiskers had been studied by SEM and HRTEM, which show that the whiskers generally have a perfect crystalline structure. Single-crystal x-ray diffraction (SCXD) patterns had been obtained along the long axis of the Sm211 whisker. These indicated that the long axis was the (001) direction. According to Zhang *et al* [16], the surfaces of the whisker appearing are the (010) planes or (110) planes. The lattice parameters are determined experimentally to be $a = 0.7253$ nm, $b = 1.2355$ nm, $c = 0.5750$ nm, $\alpha = \beta = \gamma = 90^\circ$. In the present work, we aim to systematically study the epitaxial relation between $\text{SmBa}_2\text{Cu}_3\text{O}_y$ (SmBCO) and Sm211 phase. The preferential orientation dependence of SmBCO phase on the Sm211 whisker upon supersaturation (σ) will be emphasized.

2. Experimental details

Selected whiskers were put into the sample crucible ($\varnothing 7.5$ mm \times 5 mm) of the heating stage ready for *in situ* study with a high temperature optical microscope (OLYMPUS BX51M). Some parts of the whisker were inevitably covered by Ba–Cu–O (Ba:Cu = 3:5) solvent when we picked it out from the solvent. So we used the residual flux as the solvent without additionally adding Ba–Cu–O onto the surface. Before these experiments, the temperature had been well calibrated using pure silver shavings (melting at 961 °C). All the experiments were carried out in the atmosphere and recorded by a computer attached to the high temperature optical microscope. Two different heating processes were adopted here for the *in situ* observation of the SmBCO grain growth on Sm211 whiskers. The first heating process included:

- (1) heating the sample from room temperature to 900 °C at a rate of 100 °C min⁻¹;
- (2) further increasing the temperature to 1125 °C at a rate of 10 °C min⁻¹ with a 3 min interval at 1060 °C;
- (3) then decreasing the temperature at the same rate to 1055 °C with an interval at 1060 °C for 10 min;
- (4) holding at this temperature for 10 minutes for the SmBCO crystal LPE growth;
- (5) further decreasing the temperature slowly to 1050 °C at a rate of 3 °C min⁻¹.

Unlike in the first experiment, the sample was cooled down to 1050 °C directly from 1125 °C at a fast rate of 10 °C min⁻¹ in the second experiment, where the temperature was held for 10 min. Then the temperature was increased to 1060 °C at a rate of 10 °C and held for 10 min. Lastly, the sample was cooled down to room temperature. The compositions for the different parts of the samples were determined by an EDAX detecting unit attached to the SEM.

3. Experimental results

Figure 1 is a typical SEM image showing that some grains adhere to the as-grown surface of the whiskers. These grains are almost square in shape. The magnified insets show that the grains have two preferential orientations on the whiskers. One is parallel to the long axis of

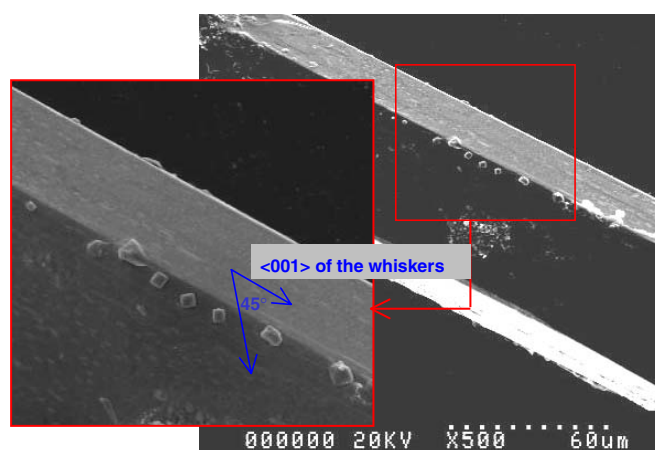


Figure 1. A typical SEM image showing some grains on the as-grown surface of the whisker with two preferential orientations: one is parallel to the long axis of the whisker, while the other is at approximately 45° to the long axis of the whisker.

the whisker, while the other is at approximately 45° to the long axis of the whisker. According to Yamada *et al* [17], the shape of the steps on the (001) face of RE123 was square and that of the steps on the (100) face was elliptical. So this indicates that some of the grains may be *c*-axis oriented SmBCO grains.

In order to confirm epitaxial growth of SmBCO grains on Sm211 whiskers, *in situ* observation by a high temperature optical microscope (HTOM) was carried out. Meanwhile, a series of compositions of the grains on SmBCO were determined by the EDAX attached to the SEM after an *in situ* experiment to confirm the formation of SmBCO phase. A typical atomic ratio of Sm:Ba:Cu corresponds to 22.94:28.62:48.45, which is different from the compositions of both Sm211 and SmBCO. As is well known, the SmBCO system is a solid solution system. In the SmBCO system, Ba is usually partially replaced by Sm atoms. This effect may be dominated by the oxygen pressure and solvent composition [18]. In this experiment, the Ba:Cu ratio may vary over a large range for different parts, which will lead to the SmBCO solid solution growth, i.e. the Ba site will be partially replaced by Sm atoms. Secondly, SmBCO crystals grew two dimensionally on Sm211 whiskers, so their thickness may be smaller than $1 \mu\text{m}$. Since the electron penetration depth is about $1 \mu\text{m}$, the composition data are inevitably influenced by the Sm211 phase. Consequently, the Sm content detected may also be enhanced. Additionally, a comparison of the composition to that of the Sm211 whiskers was made. A typical atomic ratio of Sm:Ba:Cu for the Sm211 substrate corresponds to 52.70:23.29:24.01, which is entirely different from the composition of the SmBCO phase and almost consistent with the theoretical ratio of 50:25:25 for the Sm211 phase. So it can be concluded that the epitaxially grown grains are SmBCO crystals, authentically.

A sequence of optical micrographs corresponding to the first heating process is shown in figure 2. As can be seen from figure 2(a), the morphology shows a dendritic growth of SmBCO on the Sm211 whisker for the initial few seconds at 1055°C . Subsequently, the SmBCO dendrites became regular square shapes when we held the temperature for a few minutes, as can be seen from figure 2(b). This is mainly caused by the consuming of Sm solute in the solvent, leading to a decrease of supersaturation, which makes it possible for steady growth of SmBCO grains on the whisker to occur. Additionally, the SmBCO grains grew slowly and became more regular when we decreased the temperature to 1050°C at a rate of 3°C min^{-1} ,

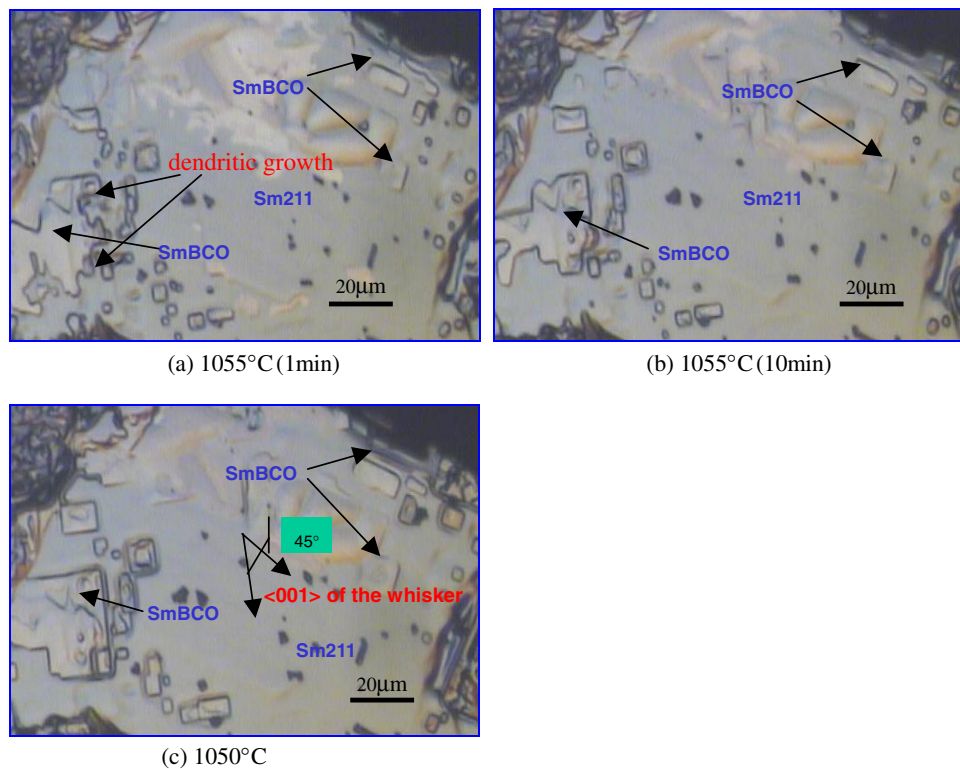


Figure 2. A series of *in situ* optical images showing the process of epitaxial growth of SmBCO on the Sm211 whisker. The coexistence of 0° and 45° SmBCO is observed *in situ*.

as shown in figure 2(c). Accordingly, it can be concluded that three factors may be attributed to the epitaxial growth of SmBCO by the peritectic reaction $\text{Sm211} + \text{L} \rightarrow \text{SmBCO}$. The first factor is a certain supersaturation of Sm solute in the solvent, which is of key importance to the nucleation and subsequent growth. The second factor is the Ba–Cu–O solvent being good for wetting the 211 phase, which makes possible continuous lateral growth of SmBCO on the Sm211 surface. The third factor is the perfect crystalline structure of the whiskers. The growth rate is greatly affected by the adsorption/desorption rate of the solute flux and the surface migration rate. For a perfect surface, the migration energy should be low, which also makes it convenient for SmBCO to grow epitaxially on the Sm211 whiskers.

Many small square-shaped SmBCO grains were also observed by a SEM and a HTOM; see figures 1 and 2, respectively. They distribute along two obvious preferential orientations: one is parallel to the whisker, and the other is at approximately 45° to the whisker. However, only one epitaxial orientation is usually expected for applications; i.e. we should encourage one direction of epitaxy growth and suppress the other at the same time. In order to achieve this, many efforts have been made. Figure 3 shows a series of optical images corresponding to the second process described in the experimental part. Figure 3(a) shows the presence of SmBCO grains on the whisker when we decreased the temperature from 1125 °C at a rate of 10 °C min⁻¹ directly to 1050 °C. Figure 3(b) shows the subsequent growth of SmBCO grains after holding the temperature at 1050 °C for about 3 min. Figures 3(c) and (d) show that these SmBCO grains began to melt at 1059 °C; a number of 0° grains remained, predominantly along the thin film growth front of SmBCO, as pointed out in figure 3(d). This is consistent

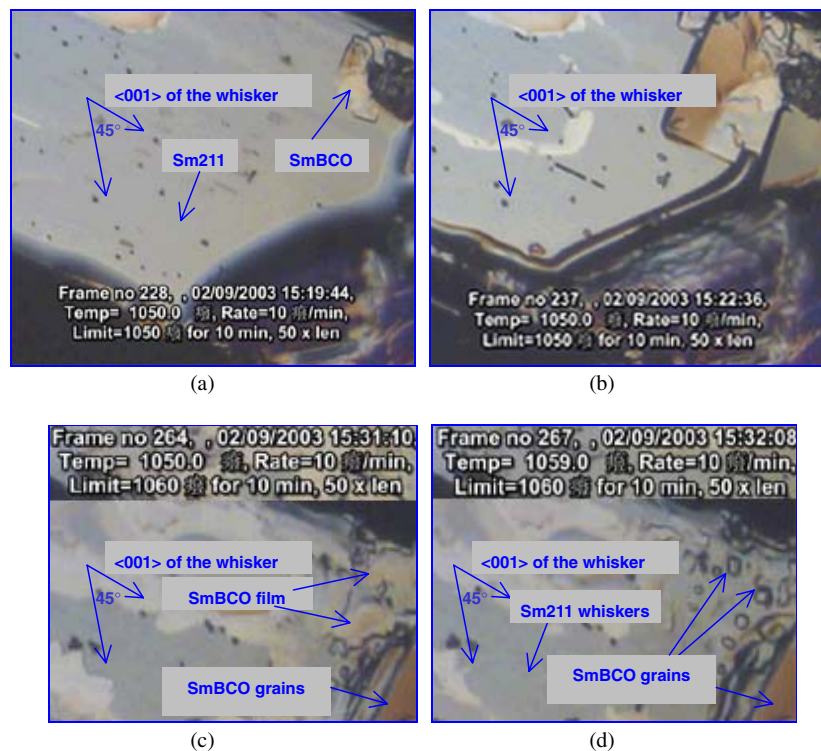


Figure 3. A series of images showing the exclusive 0° oriented SmBCO growth and melting process.

with the peritectic temperature of the SmBCO phase ($1060 \pm 10^\circ\text{C}$), which further confirms that the grains are SmBCO phase. Interestingly, only 0° oriented SmBCO grains were found in such a condition, i.e. 45° oriented SmBCO grains had been well suppressed.

4. Discussion

As we all know, there are two typical orientations for c -axis oriented Y123 crystal on MgO substrate [19]. One is $[110]_{\text{Y123}} \parallel [110]_{\text{MgO}}$, and the other is $[100]_{\text{Y123}} \parallel [110]_{\text{MgO}}$. The typical orientation relation between Y211 and MgO is $[001]_{\text{Y211}} \parallel [110]_{\text{MgO}}$ [20]. So we may consider that the Y123 phase may also have an epitaxial relation with the Y211 phase. Kim *et al* also reported the presence of preferential orientation of Y211 in the Y123 matrix [21]. SmBCO has a similar behaviour to Y123 and Sm211 is similar to Y211, so we can make a comparison. We can draw the conclusion that there may be two kinds of epitaxial orientations between SmBCO and Sm211, i.e. $[001]_{\text{Sm211}} \parallel [110]_{\text{SmBCO}}$ and $[001]_{\text{Sm211}} \parallel [100]_{\text{SmBCO}}$. Some applications will become feasible if this can be confirmed. The direct growth of SmBCO on Sm211 is one of the most attractive fields, which has potential for some applications, such as in buffer layers for coated conductors and seeds for REBCO superconductor growth, especially for the high peritectic temperature NdBCO system. However, others argued that the RE211 particles are not favoured sites for RE123 nucleation [22–25]. Nishimura *et al* suggested that the RE211 particles do not play an active role during the process of nucleation of RE123 crystals [14]. Many researchers believed that Y211 grains were grown incoherently and randomly oriented in the YBCO lattice [12, 26, 27]. So far, there is no convincing evidence to support their ideas.

Table 1. Lattice constants of SmBCO and Sm211.

	a	b	c
SmBCO	0.3844	0.3902	1.1725
Sm211	0.7253	1.2355	0.5750

Table 2. Lattice mismatch of SmBCO with different orientations on different Sm211 appearing surfaces.

(I)	Sm211	[100]	[001]	a	$2c$
0°	SmBCO	[100]	[010]	$2a$	$3b$
Mismatch				0.0600	0.0221
(II)	Sm211	[100]	[001]	$3a$	c
45°	SmBCO	[1 $\bar{1}$ 0]	[110]	$4\sqrt{a * a + b * b}$	$\sqrt{a * a + b * b}$
Mismatch				0.0069	-0.0474
(III)	Sm211	[1 $\bar{1}$ 0]	[001]	$3\sqrt{a * a + b * b}$	$2c$
0°	SmBCO	[100]	[010]	$11a$	$3b$
Mismatch				-0.0162	0.0221
(IV)	Sm211	[1 $\bar{1}$ 0]	[001]	$3\sqrt{a * a + b * b}$	c
45°	SmBCO	[1 $\bar{1}$ 0]	[110]	$8\sqrt{a * a + b * b}$	$\sqrt{a * a + b * b}$
Mismatch				0.0195	-0.0474

Accordingly, it is of great importance to clarify the orientation relationship between RE211 and RE123.

To explore this relationship, the bonding energy should be taken into considerations. As we know, the bonding energy strongly depends on the lattice matching. When the two structures have a good lattice match, their interface energy should be low. For SmBCO, the lattice constants are $a_{123} = 0.3844$ nm, $b_{123} = 0.3902$ nm, $c_{123} = 1.1725$ nm, respectively [28]. Comparing these with the lattice constants for Sm211 [15], we can see that the square root of $a_{123}^2 + b_{123}^2$ is almost equal to c_{211} , which is consistent with the orientation relationship of $[001]_{\text{Sm211}} \parallel [110]_{\text{SmBCO}}$, leading to the growth of 45° SmBCO grains. We can also find that three times a_{123} or b_{123} approximately equals two times c_{211} , which agrees well with the experimental result of $[001]_{\text{Sm211}} \parallel [100]_{\text{SmBCO}}$, leading to the growth of 0° SmBCO grains. However, with rare exceptions, epitaxy requires lattice matching in two in-plane directions. According to Zhang *et al* [16], the surfaces of the whisker appearing are the (010) planes or (110) planes. We can give an illustration on the basis of their lattice matching along two in-plane directions on these two surfaces. Table 1 lists the lattice constants of SmBCO and Sm211, and table 2 lists an illustration for the lattice matching results. (I) and (II) correspond to 0° and 45° for SmBCO on the (010) Sm211 plane, respectively, while (III) and (IV) correspond to 0° and 45° for SmBCO on the (110) Sm211 plane, respectively. From the estimated calculation, it may be suggested that the lattice matching on the Sm211 (010) plane is much better than that on the (110) plane. Accordingly, the epitaxy growth of SmBCO is more likely to take place on the (010) planes of Sm211 whisker that appear. From this analysis, 0° and 45° epitaxial orientation relations are conceivable, which accounts for the coexistence of these two kinds of grains. In the present work, an *in situ* observation confirms that both preferential orientations between SmBCO and Sm211 exist (as shown in figure 2). However, it is hard to explain the predominant growth of 0° SmBCO (as shown in figure 3) from this point of view.

In the comparison to the first process, the difference in the second experiment may result in a large supersaturation. Generally, the epitaxial growth may be considered to involve two major stages, i.e. nucleation and growth stages. In most situations, the rate-determined step is

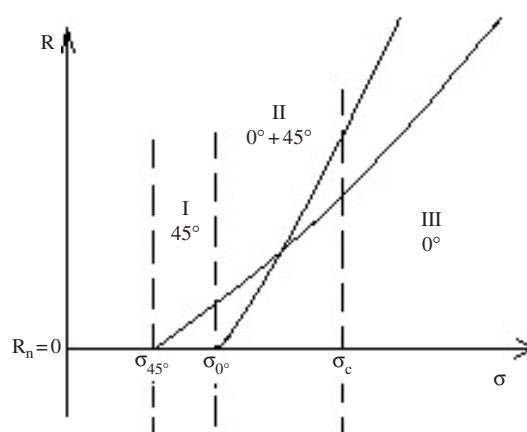


Figure 4. A schematic illustration showing the growth competition between the 0° and 45° oriented SmBCO on the Sm211 whiskers.

the first stage because the supersaturation (σ) for nucleation is usually rather larger than that for subsequent growth. The critical supersaturation for nucleation is determined by the energy of the interface, which strongly depends on the bonding energy at the interface. Furthermore, the bonding energy relates greatly to the bonding density. As analysed above, the bonding density along the 45° orientation to the $\langle 001 \rangle$ direction of the whisker is larger than that along the 0° orientation. Therefore the critical nucleation supersaturation for 45° orientation (σ_{45°) should be lower than that for 0° orientation (σ_{0°). However, the growth rate is affected by both the bonding energy at the interface and the growth habits of different SmBCO planes. It is supposed that the growth rate for 0° SmBCO may be faster than that for 45° SmBCO in some cases. As illustrated in figure 4, three cases may arise for a given supersaturation (σ). When $\sigma_{45^\circ} < \sigma < \sigma_{0^\circ}$ (I), only 45° oriented SmBCO will nucleate. Therefore, only 45° SmBCO will be found if we stabilize the supersaturation. When σ is larger than σ_{0° (II), both kinds of grains will nucleate, leading to a coexistence of 0° and 45° grains with a certain scope of σ . However, when σ reaches a critical value (σ_c), 0° and 45° SmBCO nucleate at the same time with similar nucleation rates. We can consider the bottleneck step to no longer be the nucleation stage. Correspondingly, the growth will become the rate-determined step. As supposed above, 0° SmBCO has a faster growth rate than 45° SmBCO in this condition, so after a short period of time, the 0° SmBCO grain size will be larger than that of 45° SmBCO grains. As we know, the smaller the grain size, the higher the surface energy of the grain. Hence 45° SmBCO will have a poorer stabilization than 0° SmBCO, leading to the predominant 0° SmBCO growth. Comparing the two processes, it is suggested that σ in the second experiment may be larger than that in the first experiment because of a larger temperature decrease period (directly from 1125 to 1050 °C) and a lower growth temperature (5 °C lower than the former). In short, the experimental results in figures 3 and 2 may be considered to correspond to the cases of III (0°) and II ($0^\circ + 45^\circ$), respectively. This illustration elucidates well the dominant growth of 0° SmBCO grains in the second experiment (figure 3) and the coexistence of 0° and 45° for the first experiment (figure 2).

5. Conclusion

In summary, large sized Sm211 whiskers up to 4.2 mm in length were gained by an elaborate method from the high temperature solution. The formation of SmBCO on Sm211 whiskers was

confirmed by EDS analysis. An SEM study found that SmBCO grains distributed on Sm211 whiskers along two preferential orientations of the whisker: 0° or 45° . Both preferential orientations of SmBCO and Sm211 were clarified by *in situ* observation via a high temperature optical microscope. Moreover, exclusively 0° oriented SmBCO was observed by means of rigorously controlling the heating process. A schematic illustration as regards the growth dependence of 0° and 45° SmBCO on the supersaturation was emphasized, to illustrate the preferential growth of SmBCO on Sm211 whiskers. This work will enhance our understanding of the influence of the Sm211 phase on the SmBCO phase and it also suggests some potential applications of the Sm211 phase, e.g. serving as a contamination-free buffer layer for coated conductor II.

Acknowledgments

The authors are grateful for financial support from the National Science Foundation of China (grant No 50272038), the National High Technology Research and Development Programme of China (grant No 2002AA306261), the Ministry of Education (grants Nos 20030248010 and K0293003) and Shanghai Science and Technology Committee (grant No 02DJ14041).

References

- [1] Belt R F, Ings J and Diercks G 1990 *Appl. Phys. Lett.* **56** 1805
- [2] Dubs C, Fischer K and Gönert P 1992 *J. Cryst. Growth* **123** 611
- [3] Klemmtz C and Scheel H J 1993 *J. Cryst. Growth* **129** 421
- [4] Yamada Y and Hirabayashi I 2001 *J. Cryst. Growth* **229** 343
- [5] Miura S, Hashimoto K, Wang F, Enomoto Y and Morishita T 1997 *Physica C* **278** 201
- [6] Gönert P 1997 *Cryst. Res. Technol.* **32** 7
- [7] Yamada Y 2000 *Supercond. Sci. Technol.* **13** 82
- [8] Nomura K, Hoshi S, Yao X, Nakamura Y, Izumi T and Shiohara Y 2001 *J. Mater. Res.* **16** 979
- [9] Takagi A, Wen J G, Hirabayashi I and Mizutani U 1998 *J. Cryst. Growth* **193** 71
- [10] Kakimoto K, Sugawara Y, Izumi T and Shiohara Y 2000 *Physica C* **334** 249
- [11] Asaoka H, Kazumata Y, Takei H and Noda K 1997 *Physica C* **279** 246
- [12] Sandiumenge F, Pinol S, Obradors X, Snoeck E and Roucau C 1994 *Phys. Rev. B* **50** 7032
- [13] Goyal A, Lee D F, List F A, Specht E D, Feenstra R, Paranthaman M, Cui X, Lu S W, Martin P M, Kroeger D M, Christen D K, Kang B W, Norton D P, Park C, Verebelyi D T, Thompson J R, Williams R K, Aytug T and Cantoni C 2001 *Physica C* **357** 903
- [14] Nishimura Y, Yasuhara Y, Miyashita S and Komatsu H 1996 *J. Cryst. Growth* **158** 255
- [15] Hu J, Yao X, Fu Z Q, Zeng X H and Zhang X 2005 *Supercond. Sci. Technol.* **18** 1
- [16] Zhang X, Wu X J, Yao X and Zeng X H 2004 *Mater. Charact.* **53** 1
- [17] Yamada Y, Nakamura M, Shiohara Y and Tanaka S 1995 *J. Cryst. Growth* **148** 241
- [18] Yao X, Hu J, Izumi T and Shiohara Y 2004 *J. Phys.: Condens. Matter* **16** 3819
- [19] Kakimoto K, Sugawara Y, Izumi T and Shiohara Y 2000 *Physica C* **334** 249
- [20] Yao X, Nomura K, Huang D X, Izumi T, Hobar N, Nakamura Y and Shiohara Y 2002 *Physica C* **378–381** 1209
- [21] Kim C J, Kim K B, Park H W, Kuk I H and Hong G W 1997 *J. Mater. Sci.* **32** 4701
- [22] Bataman C A, Zhang L, Chan H M and Harmer M P 1992 *J. Am. Ceram. Soc.* **75** 1281
- [23] Chen B J, Rodriguez M A, Misture S T and Synder R L 1992 *Physica C* **198** 118
- [24] Golden S J, Yamashita T, Bhargava A, Barry J C and Mackinnon I D R 1994 *Physica C* **221** 85
- [25] Reddy E S and Rajasekharan T 1998 *Phys. Rev. B* **57** 5079
- [26] Uccio U S, Granozio F M, Chiara A D, Tafuri F, Lebedev O I, Verbist K and Tendeloo G V 1999 *Physica C* **321** 162
- [27] Monot, Verbist K, Hervieu M, Laffez P, Delamare M P, Wang J, Desgardin G and Tendeloo G V 1997 *Physica C* **274** 253
- [28] Engler E M, Lee V Y and Nazzal A I 1987 *J. Am. Ceram. Soc.* **109** 2848